V. PHENOMENA OF INSTABILITY IN BINARY SYSTEMS

17. THE INSTABILITY OF SUB-GIANTS IN CLOSE BINARY SYSTEMS

ZDENĚK KOPAL
Department of Astronomy, University of Manchester, Manchester, England

I should like to open my subject by attempting to answer the following question: how many parameters are necessary and sufficient for a complete specification of the form of both components in close binary systems? Their shape should, in principle, be specified by the nature of forces acting on their surfaces, and (provided that the free period non-radial oscillations of both components are short in comparison with that of their orbits) their distortion should be governed by the equilibrium theory of tides. The level surfaces of constant density then coincide with those of constant potential, and the boundary of zero density becomes a particular case of such equipotentials.

A complete theory of the form of such surfaces for stars of arbitrary structure has not so far been developed. If, however, the density concentration inside the components of close binary systems is so high that their gravitational potentials can be approximated by those of central mass-points, the gravitational potential acting on any surface point $P(r, \theta, \phi)$ of the component of mass $\mathbf{m}_1$ should be given simply by $G(\mathbf{m}_1/r)$; the potential arising from its mate of mass $\mathbf{m}_2$ should contribute a term $G(\mathbf{m}_2/r')$, where r' denotes the distance of P from the centre of gravity of the disturbing star, and G is the constant of gravitation. The centrifugal force due to rotation with an angular velocity ω about an axis perpendicular to the orbital plane should, moreover, give rise to a contribution $\frac{1}{2}\omega^2 D^2$, where D denotes the distance of P from the axis of rotation of the distorted component. The total potential W then becomes a sum of the three components just enumerated. In close binaries it seems, moreover, reasonable to identify ω^2 with the Keplerian angular velocity $G(\mathbf{m}_1+\mathbf{m}_2)/R^3$, where R stands for the semi-major axis of the relative orbit of the two stars. Suppose now that we adopt the sum $\mathbf{m}_1+\mathbf{m}_2$ as our unit of mass, R as the unit of length, and choose the unit of time in such a way that $G=1$. If so, the desired equation of our equipotential surfaces can be shown to assume the neat form

$$C=\frac{2(1-q)}{r}+2q\left\{\frac{1}{\sqrt{1-2\lambda r+r^2}}-\lambda r\right\}+r^2(1-\nu^2)+q^2, \qquad (1)$$

where λ, μ, ν denote the direction cosines of an arbitrary radius vector r connecting P with the centre of mass of star 1, and

$$C = \frac{2RW}{G(\mathbf{m}_1 + \mathbf{m}_2)}, \qquad q = \frac{\mathbf{m}_2}{\mathbf{m}_1 + \mathbf{m}_2}, \tag{2}$$

are non-dimensional constants.

The surfaces generated by setting C = constant on the left-hand side of equation (1) can be appropriately referred to as the *Roche equipotentials*, and the C's themselves as *Roche constants*. If the latter are large, the corresponding equipotentials are known to consist of two separate ovals enclosing each one of the two mass-points, and differing but slightly from spheres. With diminishing values of C the ovals defined by (1) become increasingly elongated in the direction of the centre of gravity of the system until, for a certain critical value of $C = C_0$ (characteristic of each mass-ratio) [1], both ovals unite at a single point on the line joining the centres of the two stars. This limiting equipotential—the largest *closed* equipotential capable of containing the whole mass of the system—will hereafter be referred to as the *Roche limit*. For $C < C_0$ we can no longer regard the respective equipotentials as models of binary systems consisting of detached components, but for each value of $C \geqslant C_0$ equation (1) defines the surfaces of two distinct configurations which should describe the forms of centrally-condensed components of close binary systems, to a high degree of accuracy, *irrespective of their proximity or mass-ratio*. Therefore, the minimum number of parameters sufficient for a complete geometrical specification of *both* components in the close binary systems is *three*, and consists of the values of C_1, C_2, and q.* A properly determined trio of C_1, C_2 ($\geqslant C_0$) and q can describe the geometry of a system very much more simply and accurately than any number of artificial semi-axes of the individual components. Moreover, the quantities $C_{1,2}$ and q possess the additional advantage of a direct and simple physical meaning.

A determination of q from the spectroscopic data is sufficiently straightforward, and so is the determination of C from an analysis of the light curves [2]. Their values have recently been determined by the writer for all two-spectra eclipsing binaries of known light curves [3], and their discussion reveals that all systems possessing at least one (the more massive) component of the main sequence can be naturally divided into three groups of the following characteristics:

(*a*) *Stable Systems*. The volumes of both components are significantly

* Each one of the values of $C(\geqslant C_0)$ introduced in (1) defines, to be sure, a pair of such equipotentials for a given value of q, of which only the one enclosing the centre of gravity of the component under consideration is relevant.

smaller than their Roche limits, but their fractional dimensions and mass-ratios are such as to render the values of C for both components sensibly *equal* (in spite of the fact that the absolute values of the potential over free surfaces of the components vary from system to system by a factor in excess of ten). Both components do not deviate significantly from the main sequence in the H-R diagram, and obey statistical mass-luminosity and mass-radius relations.

(*b*) *Semi-Detached Systems*. The primary (more massive) components are significantly smaller than their Roche limits (and therefore dynamically stable), but the *secondaries* appear to fill *exactly* the largest closed equipotentials capable of containing their whole mass (i.e. $C_2 = C_0$ within the limits of observational errors). Such components lie as a rule above the main sequence, and while their primaries conform to the same mass-luminosity and mass-radius relations as stars of group (*a*), the secondary components are mostly overluminous sub-giants.

A *complementary type* of semi-detached systems, with primaries at their Roche limits and secondaries well below it (i.e. characterized by $C_1 = C_0$ and $C_2 > C_0$) *seems conspicuous by its absence*.

(*c*) *Contact Systems*. Both components appear to fill the respective loops of their Roche limits and are, therefore, probably in actual contact. Both stars lie (though not very closely) along the main sequence, but show—individually or statistically—no vestige of any relation between mass and radius or luminosity.

A schematic representation of the geometry of these three types is shown on the accompanying Fig. 1, drawn to scale for a mass-ratio $\mathbf{m}_2/\mathbf{m}_1 = 0{\cdot}6$. The question of classification of eclipsing binary systems was discussed recently at a meeting of the I.A.U. Commission 27 (Variable Stars) in connexion with the continued practice by Kukarkin and Parenago to use Algol, β Lyr, and W UMa as prototypes of such variables in their well-known *Catalogue*. It would appear now that this older system of classification has little to recommend it except tradition. The most common type of eclipsing binaries—the main sequence (stable) systems of our group (*a*) —is not recognized by it (β Aur or U Oph could be regarded as suitable prototypes). Algol itself is a typical representative of variables of our group (*b*) (semi-detached systems), while W UMa does (and β Lyr may) belong to our group (*c*). Algol and W UMa thus could be regarded as genuine prototypes of their groups, but β Lyr represents too peculiar and unique a system to be suited for the prototype of any group of common eclipsing systems. Its use in this role so far could be justified only on historical grounds, and the principal distinguishing feature between 'Algol' and

'β Lyr stars'—namely, the presence or absence of the effects of photometric ellipticity between minima—is only a matter of observational precision.

From the dynamical point of view, systems of group (*a*) should be regarded as stable unless forces other than gravitational or centrifugal are

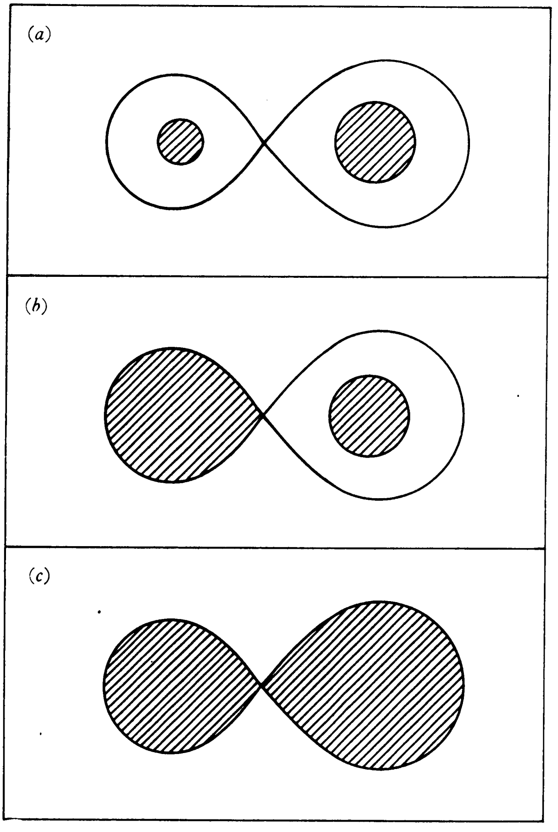

Fig. 1. A schematic view of the three principal types of close binary systems: (*a*) main sequence (stable) systems, (*b*) semi-detached systems, (*c*) contact binaries. The diagrams are drawn to scale for a mass-ratio of $\mathbf{m}_2/\mathbf{m}_1 = 0{\cdot}6$.

operative. Instability phenomena are, in principle, likely to occur among systems of group (*b*) as well as (*c*). In the present communication we shall not, however, be concerned with contact systems and propose to confine our attention to semi-detached systems whose existence is, in many respects, particularly thought-provoking. For, consider a group of well-known eclipsing systems of group (*b*), compiled in Table 1, that have been selected to demonstrate the closeness with which their secondary components cling to their Roche limits. Column 3 of this tabulation contains the values of spectroscopic mass-ratios $\mathbf{m}_2/\mathbf{m}_1$ of both components together with their observational uncertainty, and column 4 gives the diametral semi-axes of their corresponding Roche limits, taken from a recent investigation by the writer [4], their uncertainty as given being due solely to that of the mass-ratios. The last column lists then the actual diametral semi-axes of the secondary components in these systems, as deduced from an analysis of the light curves. An inspection of the data in columns 4 and 5 demonstrates that the theoretical and observed semi-axes are significantly the same in every single case, and their coincidence tends to become the closer, the smaller the uncertainty of the underlying observational data. Several other well-known systems could, moreover, be added to augment our list.

Table 1. *Fractional Dimensions of Secondary (Contact) Components in Semi-Detached Binary Systems*

Star	Spectral type	$\mathbf{m}_2/\mathbf{m}_1$	$(r_2)_{comp.}$	$(r_2)_{obs.}$
RT And B	K1	0·65 ± 0·03	0·333 ± 0·007	0·325 ± 0·004
U Cep B	gG8	0·49 ±	0·31 ±	0·31 ± 0·01
U CrB B	gG0	0·38 ± 0·01	0·290 ± 0·003	0·28 ± 0·01
u Her B	B7	0·35 ± 0·02	0·285 ± 0·004	0·287 ± 0·003
V Pup B	B3	0·58 ± 0·02	0·324 ± 0·004	0·327 ± 0·004
U Sge B	.gG6	0·30 ± 0·02	0·272 ± 0·005	0·278 ± 0·003
V 356 Sgr B	A2	0·38 ± 0·03	0·292 ± 0·007	0·28 ± 0·01
μ^1 Sco B	B6	0·66 ± 0·02	0·337 ± 0·004	0·347 ± 0·004
TX UMa B	gG4	0·30 ± 0·02	0·272 ± 0·004	0·277 ± 0·001
Z Vul B	(A2)	0·45 ± 0·02	0·303 ± 0·003	0·301 ± 0·002
RS Vul B	(F4)	0·31 ± 0·03	0·274 ± 0·007	0·26 ± 0·01

What is the significance of this clustering of secondary components in systems of this type around their Roche limits? The fact is certainly not the result of chance, for the probability of so peculiar a random distribution of fractional dimensions in so large a sample is negligibly small. It indicates rather that these stars have reached their limits by non-equilibrium processes. If they were contracting, there is no reason why any number of them should cluster around the Roche limit, but if they expand, the reason for such a clustering becomes compelling, since no larger *closed* equipotential exists which would contain their whole mass. Therefore, the growth of an expanding component of a close binary system is bound to be *arrested* at its Roche limit, and if this tendency is latent in such stars as a group, they should indeed be expected to cluster around this limit.

The observed facts just discussed can, therefore, scarcely be accounted for otherwise than by a hypothesis that the *sub-giant components in close binary systems are secularly expanding* [5]. Once the maximum distension permissible on dynamical grounds has been attained, however, a continuing tendency to expand is bound to bring about a *secular loss of mass*, by the streaming of material out of the conical end of the critical equipotential (at which the previously closed surface begins to open up). What should be the kinematic behaviour of the ejected matter once it has left the secondary component? If we ignore minor perturbations arising from the finite degree of central condensation of both components and retain the same system of units as used previously, the motion of a gas particle of negligible mass in the gravitational dipole field generated by the finite masses $\mathbf{m}_1$ and $\mathbf{m}_2$ (separated by constant distance), and referred to a rotating rectangular frame of reference whose x-axis coincides with the line joining $\mathbf{m}_1$ and $\mathbf{m}_2$ and whose y-axis lies in the plane of the orbit, should be governed by the well-known equations of the restricted problem of three bodies. Moreover, if we limit our attention to orbits in the orbital (xy-) plane, the respective equations assume the form

$$\begin{aligned} \frac{d^2x}{dt^2} - 2\frac{dy}{dt} &= \frac{\partial U}{\partial x}, \\ \frac{d^2y}{dt^2} + 2\frac{dx}{dt} &= \frac{\partial U}{\partial y}, \end{aligned} \tag{3}$$

where

$$U = \tfrac{1}{2}(x^2 + y^2) + \frac{1-q}{r} + \frac{q}{r'} \tag{4}$$

stands for the potential energy of our system. It also, incidentally, represents the rectangular–co-ordinate version of equation (1) and, at the same time, a Jacobian surface of zero velocity [6] of the moving gas particle.

The actual form of trajectories governed by the foregoing equations depends, of course, on the initial conditions of escape, and these are not yet known with any uniqueness. The locus of ejection is no doubt the conical point of the critical equipotential enclosing the less massive component (see again Fig. 1 (*b*)), identical in fact with the inner Lagrangian point L_1 at which both the velocity and acceleration of any mass particle vanish in the xy-plane. If this particle were subject to no exterior force, it would remain permanently at rest there (relative to our moving frame of reference). Conversely, an application of exterior force would require less energy to remove the particle from L_1 than from any other point on the star's surface. Concerning the nature of this force, in what follows we wish to explore the consequences of a hypothesis that the ejection is caused by a difference between the actual angular velocity ω_E of rotation at the equator of the secondary component in semi-detached binary systems, and their Keplerian angular velocity ω_K. If $\omega_E \neq \omega_K$, matter should keep moving along the equator in the xy-plane (clockwise if $\omega_E < \omega_K$, counter-clockwise if the converse is true) and, on arriving at L_1, should be ejected towards the primary (more massive) component in the direction subtending an angle with the x-axis equal to that of the osculating cone with vertex at L_1 [7]. The velocity of ejection should depend on the magnitude of $|\omega_E - \omega_K|$ and may be arbitrary within wide limits.

In order to explore the topological properties of gas streams ejected under these conditions, numerical integrations of several hundred trajectories have recently been undertaken at Manchester, for different mass-

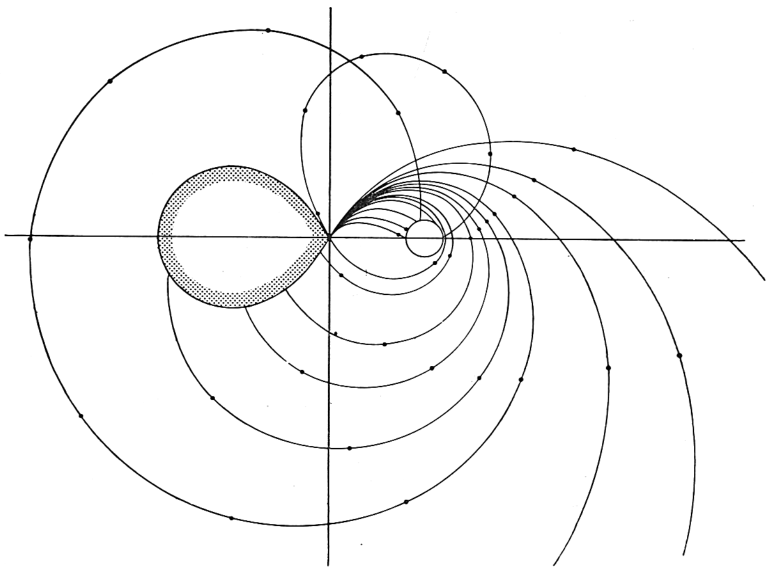

Fig. 2. Trajectories of particles ejected from L_1 with thirteen different values of the initial velocity V_0 ranging from 0·5 to 3·0, for the case of $\omega_E > \omega_K$ (direct orbits). The values of V_0 are given in Table 2. The mass-ratio $\mathbf{m}_2/\mathbf{m}_1$ is 1·0.

ratios and diverse velocities of ejection when $\omega_E \lesssim \omega_K$. These integrations have been carried out with the aid of the University of Manchester's Electronic Computers (Marks II and III) and have been programmed by my colleague R. A. Brooker of the Computing Machine Laboratory, assisted by Miss Vera Hewison of the Department of Astronomy (who is also responsible for graphical presentation of all results to be given below). The technical aspects of automatization of the differential equations of the problem of three bodies will be described by Brooker elsewhere. The aim of the present communication will be to survey the principal astronomical results obtained so far, and to give a preliminary discussion of their significance.

The accompanying Figs. 2–7 show graphical representations of the single-parameter families of the ejection orbits from L_1 for mass-ratios $\mathbf{m}_2/\mathbf{m}_1 = 1{\cdot}0$, $0{\cdot}8$, and $0{\cdot}6$, and different sets of initial velocities, the two cases $\omega_E \gtrless \omega_K$ being treated separately. On each diagram, the centre of gravity of the system is taken as the origin of co-ordinates, and the outline

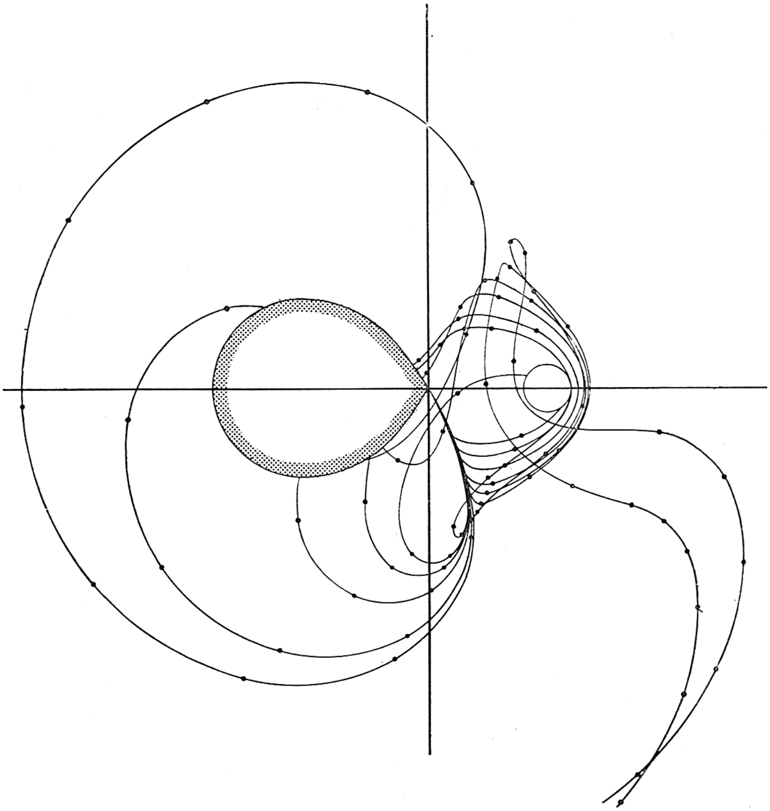

Fig. 3. Trajectories of particles ejected from L_1 with thirteen different values of the initial velocity V_0 ranging from $0{\cdot}5$ to $1{\cdot}6$, for the case of $\omega_E < \omega_K$ (retrograde orbits). The mass-ratio $\mathbf{m}_2/\mathbf{m}_1$ is $1{\cdot}0$.

of the secondary's equator is drawn to scale for the respective mass-ratio. The circle of radius $0{\cdot}1$ enclosing the primary's centre of gravity, however, merely represents a limit inside which we began getting in trouble with the scale factors of our machine integrations, rather than any anticipated size or shape of the primary component (which can be arbitrary inside its own Roche limit). Filled circles on each trajectory represent points attained by the moving particles in equal time intervals. A list of the initial velocities of all trajectories plotted on Figs. 2–7 is given in Table 2.* A great many more integrations than those shown here have been performed at Manchester to date,† but their present selection should illustrate sufficiently the main topological properties of ejection orbits (under the envisaged conditions) in the equatorial plane. Considerable work has also been done

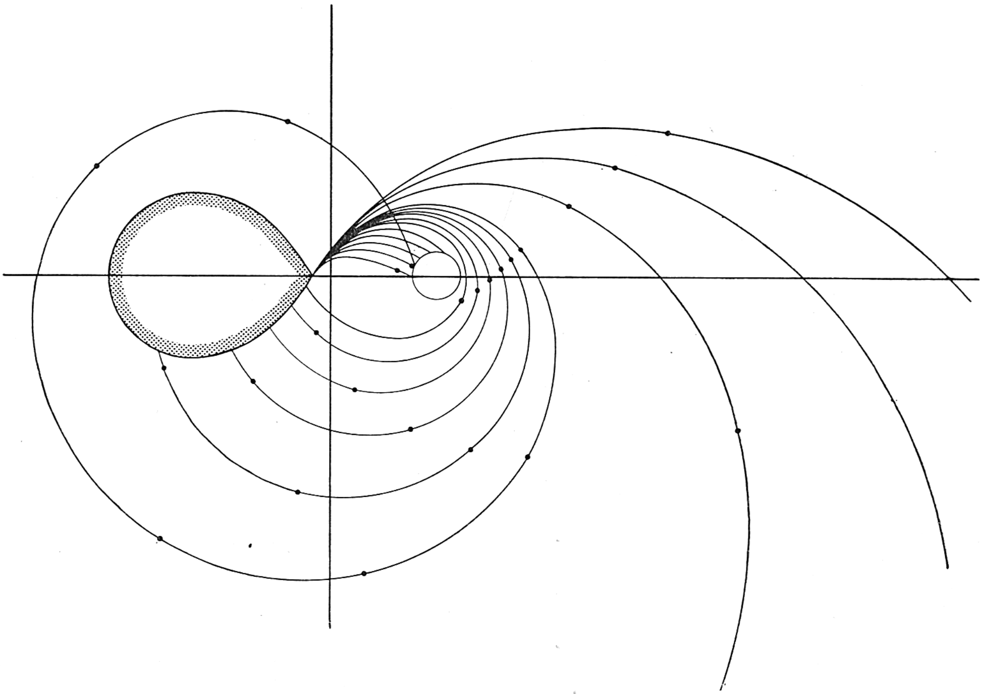

Fig. 4. Trajectories of particles ejected from L_1 with fourteen different values of the initial velocity V_0 ranging from 0·5 to 3·5, for the case of $\omega_E > \omega_K$ (direct orbits). The mass-ratio $\mathbf{m}_2/\mathbf{m}_1$ is 0·8.

on trajectories corresponding to the mass-ratio 0·4, but dynamical conditions in this latter case have proved to be considerably more complex, and a fuller presentation of the results is being postponed for a later occasion. We cannot, however, forego exhibiting on Fig. 8 at least one trajectory of this family (corresponding to the initial velocity of $v_0 = -0{\cdot}7$)‡ on account of its re-entrant character.

* The unit of velocity, consistent with our previous practice, becomes $\sqrt{G(\mathbf{m}_1+\mathbf{m}_2)/R}$ cm./sec.

† It is estimated that the machine solutions made so far are equivalent to at least 50,000 man-hours with an ordinary desk-type computing machine.

‡ In what follows, the negative sign will be used to denote velocities of ejection for $\omega_E < \omega_K$ (i.e. when y is negative), giving rise to retrograde orbits.

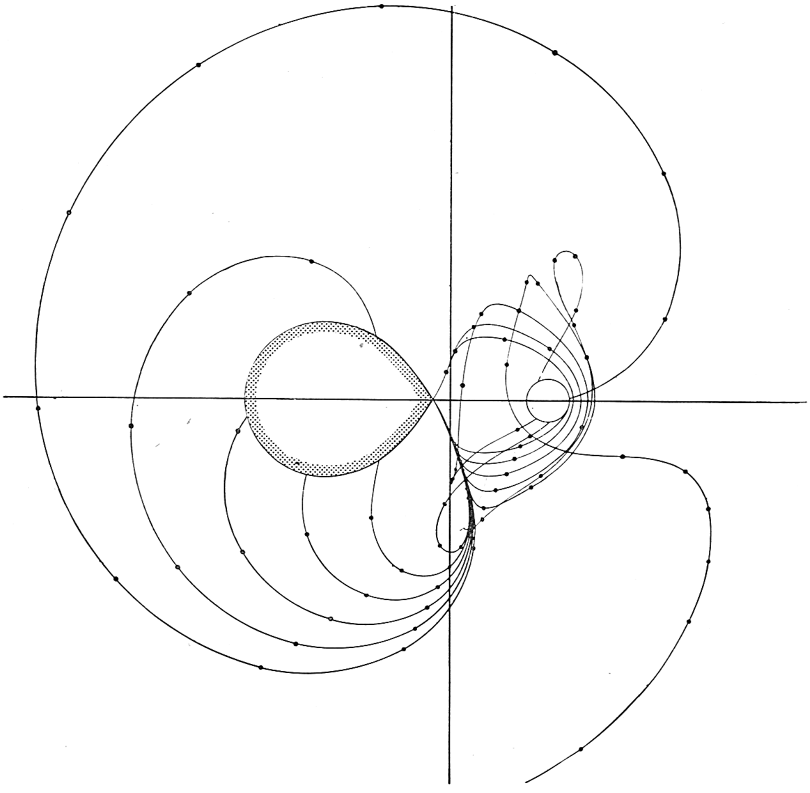

Fig. 5. Trajectories of particles ejected from L_1 with twelve different values of the initial velocity V_0 ranging from 0·5 to 1·6, for the case of $\omega_E < \omega_K$ (retrograde orbits). The mass-ratio $\mathbf{m}_2/\mathbf{m}_1$ is 0·8.

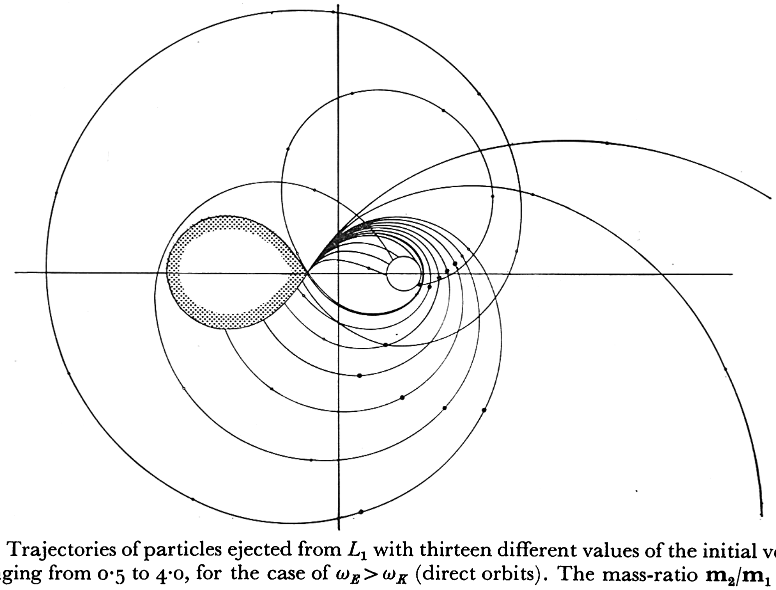

Fig. 6. Trajectories of particles ejected from L_1 with thirteen different values of the initial velocity V_0 ranging from 0·5 to 4·0, for the case of $\omega_E > \omega_K$ (direct orbits). The mass-ratio $\mathbf{m}_2/\mathbf{m}_1$ is 0·6.

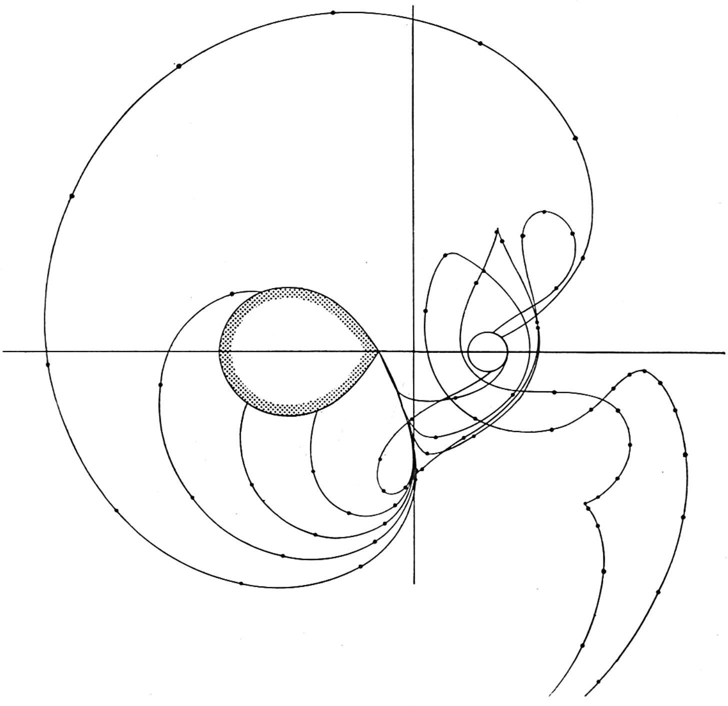

Fig. 7. Trajectories of particles ejected from L_1 with nine different values of the initial velocity V_0 ranging from 0·5 to 1·5, for the case of $\omega_E < \omega_K$ (retrograde orbits). The mass-ratio $\mathbf{m}_2/\mathbf{m}_1$ is 0·6.

Table 2. *The Initial Velocities (in Units of* $\sqrt{G(\mathbf{m}_1+\mathbf{m}_2)/R}$ *cm./sec.) of the Ejection Orbits Plotted in Figures 2–7.*

Figure:	2	4	6	3	5	7
	Direct orbits: $\omega_E > \omega_K$			Retrograde orbits: $\omega_E < \omega_K$		
$\mathbf{m}_2/\mathbf{m}_1 =$	1·0	0·8	0·6	1·0	0·8	0·6
	0·5	0·5	0·5	0·5	0·5	0·5
	0·7	0·7	0·8	0·6	0·6	0·8
	1·0	0·9	1·1	0·7	0·7	0·9
	1·3	1·1	1·4	0·8	0·8	1·0
	1·4	1·3	1·5	0·9	0·9	1·1
	1·5	1·5	1·6	1·0	1·0	1·2
	1·7	1·6	1·7	1·05	1·1	1·3
	1·8	1·7	1·8	1·15	1·2	1·4
	1·9	1·8	1·9	1·2	1·3	1·5
	2·0	1·9	2·0	1·3	1·4	—
	2·25	2·0	2·5	1·4	1·5	—
	2·5	2·5	3·0	1·5	1·6	—
	3·0	3·0	4·0	1·6	—	—
	—	3·5	—	—	—	—

The investigation outlined in this report is still in progress, and a full account of it will be published elsewhere at a later date.* The present results, incomplete as they are, lend themselves, however, to a number of tentative conclusions. If the difference $\omega_E - \omega_K$ remains moderately small (corresponding to velocities of ejection contained between $-0{\cdot}5 < V_0 < 1{\cdot}5$ for primary components of fractional radii $r = 0{\cdot}1$, and between still wider limits for larger stars),† our results leave but little room for doubt that *all matter lost by the secondary component at the inner Lagrangian point L_1 will be transferred directly to the primary star*. A continued loss of mass at L_1 due to

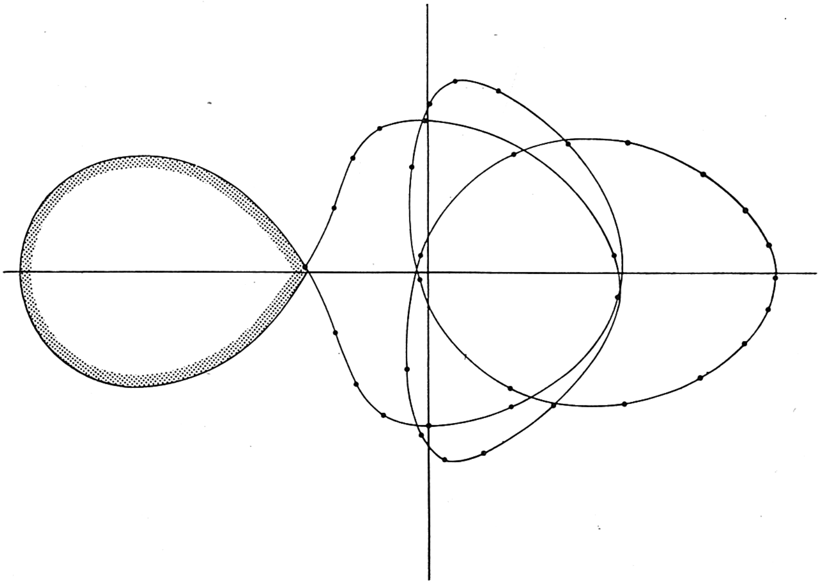

Fig. 8. Trajectory of a particle ejected from L_1 with an initial velocity of $V_0 = 0{\cdot}7$ in the case of $\omega_E < \omega_K$ (retrograde orbits), and for a mass-ratio of $\mathbf{m}_2/\mathbf{m}_1 = 0{\cdot}4$.

secular expansion of the secondary component is, therefore, in time bound to keep increasing the disparity in masses between the two components of the same pair. Now close eclipsing systems with sub-giant secondaries have long been known to exhibit abnormally large mass-ratios—a fact discussed particularly by Struve [8]. As most (if not all) such companions have been found to possess fractional dimensions coinciding with their Roche limits, there remains but little room for doubt that the relative smallness of their present masses is but the consequence of a secular transfer of mass from the

* We shall, however, be pleased to furnish particular results, in advance of publication, to any investigator who may request them.

† It should be stressed that, in most binary systems, the actual velocities of ejection are likely to lie within these limits.

secondary to the primary components by 'gravitational pipelines' shown on our Figs. 2–7.

If the velocity of ejection becomes higher (its exact limit depending on the size of the primary component), the mass ejected at L_1 may circumnavigate the primary component and be intercepted by the secondary

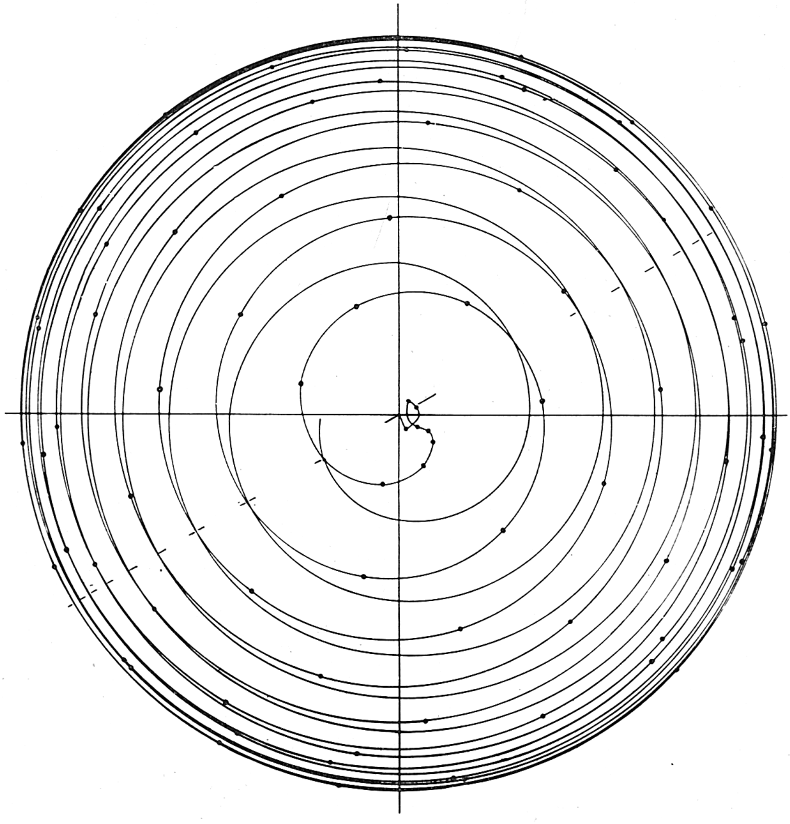

Fig. 9. Trajectory of a particle ejected from L_1 with an initial velocity of $V_0 = 0{\cdot}9$ in the case of $\omega_E < \omega_K$ (a retrograde orbit), and for a mass-ratio $\mathbf{m}_2/\mathbf{m}_1 = 1{\cdot}0$. The scale is more compressed than that of Figs. 2–7.

anywhere along its equator (cf. again Figs. 2–7), or, with further increase of ejection speed, circumnavigate the primary *and* secondary until falling at last on the primary star. It is not until still higher velocities are attained—velocities much higher than the radial velocities of any gas streams actually observed in eclipsing variables (with the possible exception of β Lyrae, or of the Wolf-Rayet and other anomalous binaries)—that matter ejected by the secondary component at L_1 can actually spiral out in the equatorial plane and be lost to the system. In fact, one of the principal results of the present investigation is the full realization of the difficulty with which any matter can be permanently expelled from a close binary system.*

If $\omega_E > \omega_K$, the foregoing description covers broadly any dynamical contingency which may arise, but for $\omega_E < \omega_K$ an additional interesting possibility should be mentioned in this connexion: namely, the existence of a class of retrograde orbits corresponding to a relatively narrow initial-

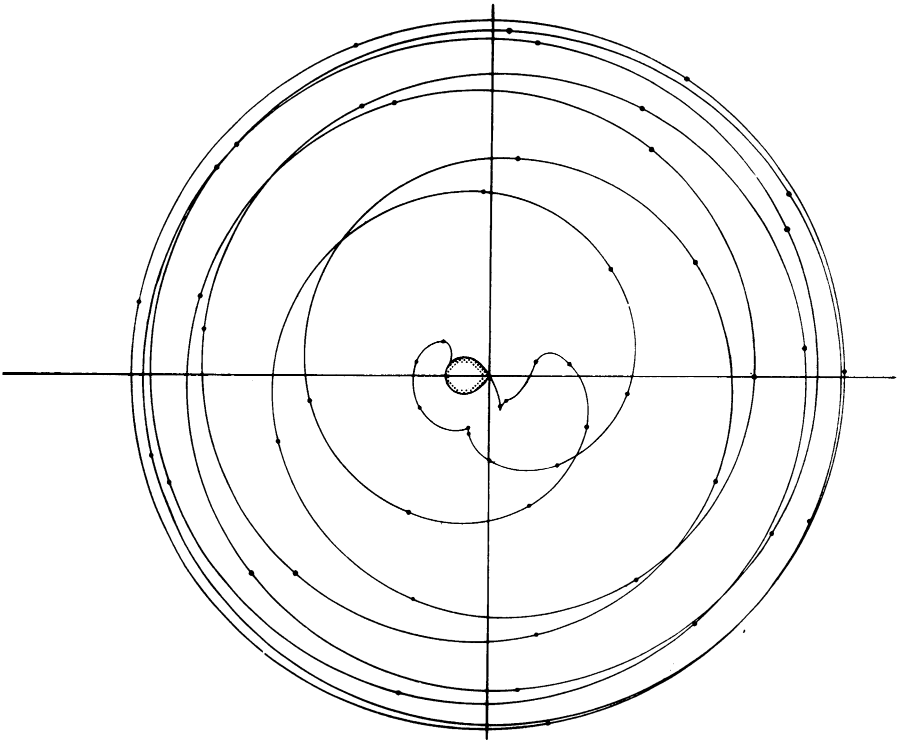

Fig 10. Trajectory of a particle ejected from L_1 with an initial velocity of $V_0 = 1 \cdot 0$ in the case of $\omega_E < \omega_K$ (a retrograde orbit), and for a mass-ratio $\mathbf{m}_2/\mathbf{m}_1 = 1 \cdot 0$. The scale is more compressed than that of Figs. 2–7. Fig. 3 should be consulted for the details of the inner part of the trajectory.

velocity range around $V_0 = -1 \cdot 0$. Our numerical integrations show (cf. Figs. 3, 5 and 7) that the particles departing from L_1 with such a velocity may, after circumnavigating the primary component (and describing cusps in the neighbourhood of the Lagrangian equilateral points L_4 and L_5), pass through the gap between the two stars and recede thereafter to a considerable distance from the system. In two cases (corresponding to the mass-ratio 1·0 and the ejection velocities $V_0 = -0 \cdot 9$ and $-1 \cdot 0$), we have

* The opening-up of the corresponding Jacobian surface of zero velocity is a necessary, but not sufficient, condition for such an escape.

followed the orbits of such particles for many thousands of steps (requiring integrations which took hours to perform even at electronic speeds).

The outcome, plotted on Figs. 9 and 10 on a much reduced scale, reveals that the recession of a particle from its parent binary system does not continue indefinitely, but possesses an upper limit (of radius about ten times as large as the radius of the orbit of the two finite bodies), which our particle will approach asymptotically before it will eventually spiral inward to end its motion by falling on one of the two components. The asymptotic nature of the orbit (cf., in particular, Fig. 9) suggests that a continuous stream of particles moving along it may lead to the maintenance of a distinct gas ring, encircling the whole binary system at a considerable distance from it and (as indicated by the time-dots) rotating with respect to it with almost constant angular velocity. Now the existence of gaseous rings of this nature, encircling certain eclipsing systems, has indeed been reported by several investigators. Whether or not these are dynamically related to the secondary component by particle orbits discussed in this paper, however, remains to be settled by future investigations.

REFERENCES

[1] For their tabulation cf. Kopal, Z., *Jodrell Bank Ann.* **1**, 37 (1954) (Table V, col. 2).

[2] Details of this process are being postponed for subsequent publication.

[3] The material at the basis of this study is summarized in Table V of the Draft Report prepared by the writer on behalf of Commission 42 of the I.A.U. for the 9th General Assembly in Dublin, and will be published in the *I.A.U. Transactions*, vol. **9**.

[4] Cf. Kopal, Z., *Jodrell Bank Ann.* **1**, 37 (1954) (Table I, col. 7).

[5] This conclusion, announced by the writer at the sixth International Astrophysical Colloquium at Liège in July 1954 (cf. *Communications presentées au sixième Colloque International d'Astrophysique*, Liège, 1955, pp. 684–5), was independently arrived at by J. A. Crawford [*Ap.J.* **121**, 71 (1955)] on the basis of a statistical study of completely different material.

[6] For fuller details cf., e.g., F. R. Moulton, *An Introduction to Celestial Mechanics* (6th ed., New York, 1939) chapter VIII, sec. 154.

[7] These angles have been tabulated for different mass-ratios by Kopal in *Jodrell Bank Ann.* **1**, 37 (1954) (Table III).

[8] Struve, O., *Ann. d'Ap.* **11**, 117 (1948); also *Harvard Centennial Symposia* (*Harv. Obs. Mono.* No. 7, Cambridge, 1948), pp. 211–30.